J. Fluid Mech. (1976), *vol.* 77, *part* 4, *pp.* 665–684
Printed in Great Britain

The moving contact line: the slip boundary condition

By E. B. DUSSAN V.

Department of Chemical and Biochemical Engineering,
University of Pennsylvania, Philadelphia

(Received 1 December 1975)

The singularity at the contact line which is present when the usual fluid-mechanical modelling assumptions are made is removed by permitting the fluid to slip along the wall. The aim of this study is to assess the sensitivity of the overall flow field to the form of the slip boundary condition. Explicit solutions are obtained for three different slip boundary conditions. Two length scales emerge: the slip length scale and the meniscus length scale. It is found that on the slip length scale the flow fields are quite different; however, when viewed on the meniscus length scale, i.e. the length scale on which almost all fluid-mechanical measurements are made, all of the flow fields appear the same. It is found that the characteristic of the slip boundary condition which affects the overall flow field is the magnitude of the slip length.

1. Introduction

A contact line is located at the intersection of a fluid–fluid interface (formed by two immiscible fluids) and a solid bounding wall. A *moving* contact line can be found in many different situations; some cases in which it plays a central role are the spreading of adhesives, the flowing of lubricants into inaccessible locations, the coating of solid surfaces with a thin uniform layer of liquid, the displacement of oil by water through a porous medium, etc. However, the dynamics of the fluid surrounding the contact line, and hence the contact line itself, are poorly understood. Dussan V. & Davis (1974) have shown that the difficulty arises from the fact that the usual fluid-mechanical modelling assumptions break down in this region, hence a proper model for the fluids near the moving contact line is not known. They have shown that if the fluids are Newtonian and incompressible and do not slip along the rigid bounding surface (the fluids are also assumed to undergo a generalized rolling-type motion) then unbounded forces are produced at the contact line (refer to the article for a precise statement). Such a singularity is present in the flow field given by Huh & Scriven (1971), which was obtained under more restrictive conditions. Ludviksson & Lightfoot (1968) avoided these difficulties by assuming that the surface is prewetted by the spreading fluid. In part they were motivated by the observations of Bascom, Cottington & Singleterry (1964), who detected a very thin primary film (less than 100×10^{-10} m thick) spreading ahead of a thicker secondary film (approximately 10^{-6} m thick) in a system consisting of squalane spreading up a vertical smooth steel plate surrounded by air. On the other hand, if Ludviksson & Lightfoot had not assumed

the presence of a thin film then their equation for the shape of the fluid–fluid interface would have been singular at the contact line. Lopez, Miller & Ruckenstein (1976) included in their analysis a body force which models long-range molecular forces. Upon making the lubrication approximation they derived an expression for the shape of a spreading two-dimensional drop; however it has the characteristic that the fluid–fluid interface does not make contact with the solid surface. Since their body force can be written as a gradient of a scalar and the fluid was assumed incompressible, the results of Dussan V. & Davis (1974) can be used to conclude that such a fluid exerts an unbounded force at the moving contact line, if it is assumed that the contact line exists (this conclusion is independent of the lubrication approximation).

Since the proper model (or models, since there is probably more than one mechanism responsible for spreading) for the fluids adjacent to the moving contact line is not yet known, one can proceed along two different, although complementary, paths: (i) derive models based upon non-equilibrium statistical mechanics; (ii) make *ad hoc* continuum modelling assumptions, solve the associated well-posed boundary-value problems and examine their effect on the overall flow field. It is the latter approach which we shall pursue. It will be assumed that the fluids are incompressible and Newtonian, and the singularity will be removed by permitting the fluid to slip along the wall in the immediate vicinity of the moving contact line. The aim of this investigation is to determine how great an effect the specific details of the slip model have on the motion of the fluid when it is examined on length scales used by fluid mechanicians. Since it removes a singularity which is responsible for an unbounded force and undefined interfacial shape, we know already that its presence will be detectable. However, one should keep in mind that no relevant experiments have been performed to document slip for slow flow near a moving contact line. Huh & Scriven (1971) have suggested, among a long list of other things, permitting the fluid to slip near the moving contact line; however they were motivated by the misconception that the no-slip boundary condition and the mutual displacement of two viscous fluids along a solid wall are kinematically incompatible concepts.

In § 2 the motion of the fluid near the moving contact line formed when a plate is removed at an arbitrary angle from a semi-infinite domain of fluid is analysed. In order to make the problem tractable, the velocity and pressure fields and the shape of the free surface (since there is no second fluid the fluid–fluid interface is called a free surface) are expanded in terms of the Reynolds number, the capillary number and the critical static contact angle. The analysis is limited to cases in which the critical static contact angle is close but not necessarily equal to the angle at which the plate is removed from the fluid. The solution for the velocity field, to lowest order, is obtained in terms of an arbitrary slip velocity along the plate by using the Mellin transformation. Three specific slip boundary conditions are investigated and exact explicit expressions are obtained for their corresponding velocity fields for the case when the plate is removed at an angle of 90° (a solution for an arbitrary angle is presented in the appendix). In § 3 the lowest-order dynamic contribution to the shape of the free surface is calculated exactly in terms of an integral which must be evaluated

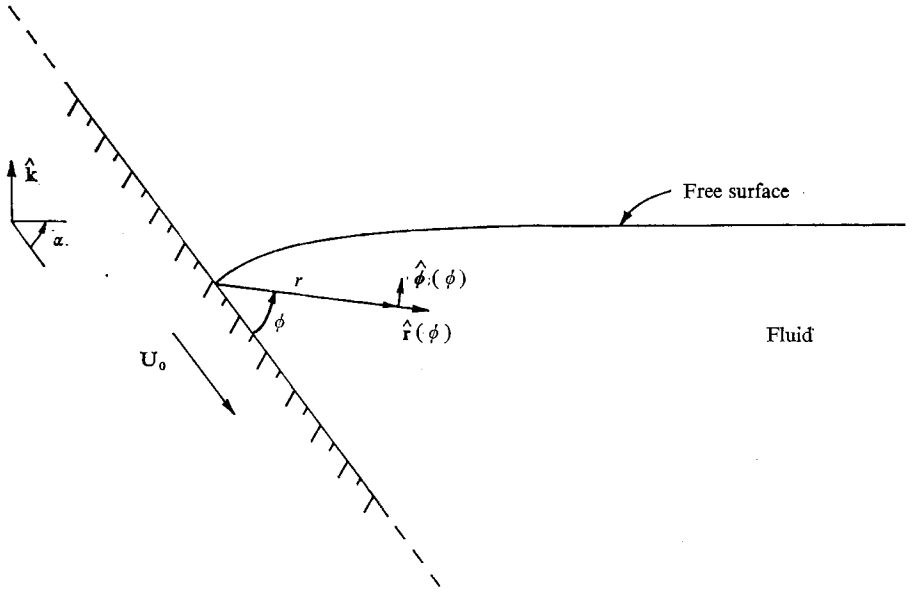

FIGURE 1. A plate inclined at an angle α with respect to the horizontal is inserted into a field. The free surface is assumed to approach a flat horizontal configuration far away from the plate.

numerically, and approximately by performing an asymptotic expansion in terms of the Bond number about a singular limit. The results and conclusions appear in §§ 4 and 5, respectively.

2. Analysis

A plate of infinite extent is either inserted into or withdrawn from a semi-infinite domain of fluid at a constant velocity $\mathbf{U}_0$ (figure 1). The flow is assumed to be two-dimensional and steady, and the geometry of the free surface is assumed to be stationary, all with respect to our frame of reference. The contact line, even though it appears to be at rest, is considered to be moving owing to its relative motion with respect to the plate. A polar co-ordinate system is used whose origin is located at the contact line.

The equations of motion and boundary conditions in dimensionless form are: the Navier–Stokes equation

$$Re\frac{d\mathbf{u}}{dt} = -\frac{\nabla P}{C} + \nabla^2\mathbf{u} - \frac{B}{C}\hat{\mathbf{k}};$$

the equation of continuity

$$\nabla.\mathbf{u} = 0;$$

the kinematic boundary conditions

$$\mathbf{u}.\hat{\boldsymbol{\phi}} = 0 \quad \text{on} \quad \phi = 0, \tag{2.1}$$

$$\mathbf{u}.\mathbf{n} = 0 \quad \text{on} \quad \phi = \phi(r), \tag{2.2}$$

where $\mathbf{n}$ is a unit outward normal to the free surface, which is located at $\{(r, \phi(r)) | 0 \leqslant r < \infty\}$; the dynamic boundary conditions

$$\boldsymbol{\tau} . \mathbf{T} . \mathbf{n} = 0 \quad \text{on} \quad \phi = \phi(r), \tag{2.3}$$

where $\mathbf{T}$ is the stress tensor and $\boldsymbol{\tau}$ is a unit tangent vector to the free surface, i.e. $\boldsymbol{\tau} . \mathbf{n} = 0$, and

$$\mathbf{n} . \mathbf{T} . \mathbf{n} = \frac{1}{r} \frac{d}{dr} \left(r^2 \frac{d\phi}{dr} \right) + r^2 \left(\frac{d\phi}{dr} \right)^3 \Big/ \left\{ 1 + \left(r \frac{d\phi}{dr} \right)^2 \right\}^{\frac{3}{2}} \quad \text{on} \quad \phi = \phi(r); \tag{2.4}$$

the slip boundary condition

$$\mathbf{u} = U(r) \hat{\mathbf{r}} \quad \text{on} \quad \phi = 0, \tag{2.5}$$

where $U(r)$ is a prescribed function; and that the critical static contact angle

$$\phi(0) = \phi_s, \tag{2.6}$$

where ϕ_s is either the advancing or the receding static contact angle depending on whether $\mathbf{U}_0 . \hat{\mathbf{r}}(0)$ is positive or negative (these angles are defined to be the static angles approached in the limit as $|\mathbf{U}_0| \to 0$). The fact that these two contact angles differ, often referred to as contact-angle hysteresis, has been documented experimentally and is widely accepted; the reason for the difference is not known, although there are many speculations (Zisman 1964; Johnson & Dettre 1964). The specific set of functions assumed for $U(r)$ appears after (2.15). The rationale behind this choice and the diversity represented by this set are discussed at the beginning of §§ 4 and 5.

The dimensional forms of the variables appearing in the above equations are

$$\mathbf{u} U_0, \quad P\sigma/L_s, \quad \mathbf{T}\sigma/L_s, \quad r L_s, \quad L_s t/U_0,$$

where $U_0 \equiv \mathbf{U}_0 . \hat{\mathbf{r}}(0)$ is the speed of the plate, σ is the surface tension and L_s is the slip length (its exact definition is intimately related to $U(r)$ in (2.5) and it will be discussed in more detail later). The parameters are the Reynolds number $Re \equiv U_0 L_s/\nu$, the capillary number $C \equiv U_0 \mu/\sigma$, the Bond number $B \equiv \rho g L_s^2/\sigma$, the angle between the free surface far from the wall and the wall, $\alpha \equiv \lim_{r \to \infty} \phi(r)$, and the normalized critical static contact angle $\epsilon \equiv (\phi_s - \alpha)/\alpha$.

The dependent variables are expanded asymptotically in Re, C and ϵ in the limit as each parameter approaches zero:

$$\begin{Bmatrix} \mathbf{u} \\ P \\ \phi \end{Bmatrix} \sim \begin{Bmatrix} \mathbf{u}_{000}(r, \phi; B) \\ P_{000}(r, \phi; B) \\ \phi_{000}(r; B) \end{Bmatrix} + \epsilon \begin{Bmatrix} \mathbf{u}_{001}(r, \phi; B) \\ P_{001}(r, \phi; B) \\ \phi_{001}(r; B) \end{Bmatrix} + C \begin{Bmatrix} \mathbf{u}_{010}(r, \phi; B) \\ P_{010}(r, \phi; B) \\ \phi_{010}(r; B) \end{Bmatrix} + Re \begin{Bmatrix} \mathbf{u}_{100}(r, \phi; B) \\ P_{100}(r, \phi; B) \\ \phi_{100}(r; B) \end{Bmatrix} + \ldots .$$

The above expansions simplify the problem in the following way: the expansion in Re linearizes the Navier–Stokes equation; the expansion in C gives rise to a domain perturbation for the free surface about its static configuration, and the expansion in ϵ gives rise to a static free-surface profile which is close to the curve

$\phi = \alpha$. Later, when solving for the shape of the free surface, an expansion will also be made in B in the limit as $B \to 0$; however in this case the expansion is singular.

Lowest order

The Navier–Stokes equation and the dynamic boundary condition (2.4) give

$$0 = -\nabla P_{000} - B\hat{\mathbf{k}}$$

and $P_{000}(r, \alpha) = 0$ with $\phi_{000}(r; B) = \alpha$. The solution for P_{000} is

$$P_{000} = -Br\sin(\phi - \alpha).$$

To lowest order the fluid is static and in a wedge configuration.

First order

Again, to this order the fluid is static. The Navier–Stokes equation and the dynamic boundary condition (2.4) give

$$0 = \nabla P_{001}$$

and

$$\frac{1}{r}\frac{d}{dr}\left(r^2\frac{d\phi_{001}}{dr}\right) = rB\phi_{001} - P_{001},$$

subject to the conditions given by (2.6) that

$$\phi_{001}(0; B) = \alpha$$

and that the free surface becomes horizontal as $r \to \infty$, i.e.

$$\lim_{r\to\infty}\frac{1}{r}\frac{d}{dr}\left(r^2\frac{d\phi_{001}}{dr}\right) = 0.$$

The solution to the above is

$$\phi_{001} = \frac{\alpha}{B^{\frac{1}{2}}}\left(\frac{1 - e^{-B^{\frac{1}{2}}r}}{r}\right), \quad P_{001} = \alpha B^{\frac{1}{2}}.$$

The static configuration given by the sum of the above and the lowest-order mode corresponds to the configuration attained in the limit as $\mathbf{U}_0 \to 0$.

Second order

This is the lowest order at which the fluid is in motion. The Navier–Stokes equation and the continuity equation give

$$0 = -\nabla P_{010} + \nabla^2\mathbf{u}_{000}, \quad \nabla.\mathbf{u}_{000} = 0. \qquad (2.7), (2.8)$$

The kinematic boundary conditions (2.1) and (2.2) give

$$\mathbf{u}_{000}.\hat{\boldsymbol{\phi}} = 0 \quad \text{on} \quad \phi = 0, \alpha, \qquad (2.9), (2.10)$$

while the dynamic boundary conditions (2.3) and (2.4) give

$$r\frac{\partial}{\partial r}\left(\frac{v_{000}}{r}\right) + \frac{1}{r}\frac{\partial u_{000}}{\partial \phi} = 0 \quad \text{on} \quad \phi = \alpha \qquad (2.11)$$

and

$$\frac{1}{r}\frac{d}{dr}\left(r^2\frac{d\phi_{010}}{dr}\right) = r\phi_{010}B - P_{010} + 2\left(\frac{1}{r}\frac{\partial v_{000}}{\partial\phi} + \frac{u_{000}}{r}\right) \quad \text{on} \quad \phi = \alpha, \tag{2.12}$$

where $\mathbf{u}_{000} = u_{000}\hat{\mathbf{r}} + v_{000}\hat{\boldsymbol{\phi}}$. The slip boundary condition (2.5) gives

$$u_{000} = U(r) \quad \text{on} \quad \phi = 0. \tag{2.13}$$

The aim is to obtain a solution to the above well-posed problem.

The solution of the second-order problem separates into two parts: first, one seeks a solution for the velocity field [this involves (2.7)–(2.11) and (2.13)] which is unaffected by the form of the body force as long as it is conservative; second, one solves (2.12) for the shape of the free surface. In order to obtain the general solution for the velocity field we proceed in the usual way and introduce the stream function ψ: $(u_{000}, v_{000}) = (-r^{-1}\partial\psi/\partial\phi, \partial\psi/\partial r)$. Taking the curl of (2.7) gives the governing equation for ψ, the biharmonic equation:

$$\left\{\frac{1}{r}\frac{\partial}{\partial r}r\frac{\partial}{\partial r} + \frac{1}{r^2}\frac{\partial^2}{\partial\phi^2}\right\}^2\psi = 0.$$

The boundary conditions given by (2.9)–(2.11) and (2.13) become

(i) $\psi = 0$ on $\phi = 0$,

(ii) $\psi = 0$ on $\phi = \alpha$,

(iii) $\partial^2\psi/\partial\phi^2 = 0$ on $\phi = \alpha$,

(iv) $\partial\psi/\partial\phi = -rU(r)$ on $\phi = 0$.

A solution to the above is sought by using Mellin transformations (Morse & Feshbach 1953, p. 469):

$$\overline{\psi}(s,\phi) \equiv \mathscr{M}(\psi) \equiv \int_0^\infty \psi(r,\phi)\, r^{s-1}dr, \tag{2.14a}$$

$$\psi(r,\phi) \equiv \mathscr{M}^{-1}(\psi) \equiv \frac{1}{2\pi i}\lim_{R\to\infty}\int_{\sigma_0-iR}^{\sigma_0+iR}\overline{\psi}(s,\phi)\, r^{-s}ds, \tag{2.14b}$$

where σ_0 is determined by the boundary conditions. The transformed biharmonic equation and boundary conditions are

$$d^4\overline{\psi}/d\phi^4 + [s^2 + (s+2)^2]\, d^2\overline{\psi}/d\phi^2 + (s+2)^2 s^2\overline{\psi} = 0,\dagger$$

(i) $\overline{\psi} = 0$ on $\phi = 0$,

(ii) $\overline{\psi} = 0$ on $\phi = \alpha$,

(iii) $d^2\overline{\psi}/d\phi^2 = 0$ on $\phi = \alpha$,

(iv) $d\overline{\psi}/d\phi = F(s) \equiv \mathscr{M}(-rU(r))$ on $\phi = 0$.

The solution for $\overline{\psi}$ is

$$\overline{\psi}(s,\phi) = \frac{F(s)\{\sin s\alpha \sin[(s+2)(\phi-\alpha)] - \sin(s+2)\alpha \sin s(\phi-\alpha)\}}{-(s+1)\sin 2\alpha + \sin(s+1)2\alpha}. \tag{2.15}$$

† Tranter (1948) uses Mellin transforms to solve for the stress within an infinite wedge-shaped elastic body which is subjected to known surface tractions on its boundary. The governing equation is also the biharmonic equation.

Solutions are sought for $\alpha = \frac{1}{2}\pi$ and for three different slip boundary conditions $U(r)$:

$$U_1 \equiv \frac{r}{1+r}, \quad U_2 \equiv \frac{r^2}{1+r^2}, \quad U_{\frac{1}{2}} \equiv \frac{r^{\frac{1}{2}}}{1+r^{\frac{1}{2}}}.$$

All of these slip boundary conditions have the characteristic that the no-slip condition is approached as one moves away from the immediate vicinity of the contact line, i.e. $\lim_{r\to\infty} U_i = 1$ for $i = 1, 2$ and $\frac{1}{2}$.

The inverse Mellin transform is obtained by the technique of summing residues. An outline of the calculations for the specific case $U(r) = U_1$ follows.

The transform of the slip velocity gives

$$F_1(s) = -\pi \operatorname{cosec} \pi s,$$

with the restriction that $-2 < \sigma_0 < -1$, where $\sigma_0 = \operatorname{Re} s$ [see (2.14*b*)]. The stream function in transform space is

$$\overline{\psi}_1 = \frac{\pi \cos(\phi - \frac{1}{2}\pi) \sin[(s+1)(\phi - \frac{1}{2}\pi)]}{2\cos^2 \frac{1}{2}s\pi \sin \frac{1}{2}s\pi},$$

which is analytic in s except at simple poles at $0, -1, \pm 2, \pm 4, \ldots$ and double poles at $+1, \pm 3, \pm 5, \ldots$. The Cauchy integral theorem enables us to write

$$\frac{1}{2\pi i}\int_{\sigma_0 - iR_N}^{\sigma_0 + iR_N} \overline{\psi}_1(s, \phi) r^{-s} ds = -\sum_{n=-1}^{N} \operatorname{Res}(\overline{\psi}_1 r^{-s} | s = n) - \frac{1}{2\pi i}\int_{\mathscr{C}} \overline{\psi}_1(s, \phi) r^{-s} ds,$$

where $R_N = N + \frac{1}{2}$ and $\mathscr{C}$ consists of a semicircle of radius R_N with centre at $s = 0$ and located in the half-plane $\operatorname{Re} s \geqslant 0$ and two straight line segments $\{\sigma + i\tau | \sigma_0 \leqslant \sigma \leqslant 0; \tau = \pm R_N\}$. It can easily be shown that for $r > 1$

$$\lim_{N\to\infty} \int_{\mathscr{C}} \overline{\psi}_1(s, \phi) r^{-s} ds = 0.$$

This gives

$$\psi_1(r, \phi) = -\sum_{n=-1}^{\infty} \operatorname{Res}(\overline{\psi}_1 r^{-s} | s = n),$$

or, equivalently,

$$\begin{aligned}\psi_1(r, \phi) = &-\cos(\phi - \tfrac{1}{2}\pi) \sum_{\substack{n=0 \\ n \text{ even}}}^{\infty} (-1)^{\frac{1}{2}n} r^{-n} \sin(n+1)(\phi - \tfrac{1}{2}\pi) \\ &+ 2\pi^{-1} \cos(\phi - \tfrac{1}{2}\pi) \sum_{\substack{n=1 \\ n \text{ odd}}}^{\infty} (-1)^{\frac{1}{2}(n-1)} r^{-n} \{(\ln r) \sin(m+1)(\phi - \tfrac{1}{2}\pi) \\ &- (\phi - \tfrac{1}{2}\pi) \cos(n+1)(\phi - \tfrac{1}{2}\pi)\} + 2\pi^{-1} r(\phi - \tfrac{1}{2}\pi) \cos(\phi - \tfrac{1}{2}\pi).\end{aligned}$$

Summing the series gives an expression valid for $0 < r < \infty$:

$$\begin{aligned}\psi_1(r, \phi) = &-\tfrac{1}{2}\sin 2(\phi - \tfrac{1}{2}\pi) + 2r\pi^{-1}(\phi - \tfrac{1}{2}\pi)\cos(\phi - \tfrac{1}{2}\pi) \\ &+ \frac{r\cos(\phi - \frac{1}{2}\pi)\{r^{-3}\sin 3(\phi - \frac{1}{2}\pi) + r^{-5}\sin(\phi - \frac{1}{2}\pi)\}}{1 + 2r^{-2}\cos 2(\phi - \frac{1}{2}\pi) + r^{-4}} \\ &- \frac{2}{\pi}\frac{\cos(\phi - \frac{1}{2}\pi)\{(\phi - \frac{1}{2}\pi)(r^{-1}\cos 2(\phi - \frac{1}{2}\pi) + r^{-3}) - r^{-1}(\ln r)\sin 2(\phi - \frac{1}{2}\pi)\}}{1 + 2r^{-2}\cos 2(\phi - \frac{1}{2}\pi) + r^{-4}}.\end{aligned}$$

In a similar manner we solve for the stream functions ψ_2 and $\psi_{\frac{1}{2}}$ associated with the slip boundary conditions $U(r) = U_2$ and $U_{\frac{1}{2}}$, respectively. The Mellin transforms of U_2 and $U_{\frac{1}{2}}$ are

$$F_2(s) = +\tfrac{1}{2}\pi \operatorname{cosec} \tfrac{1}{2}\pi(s+1) \quad \text{with} \quad -3 < \sigma_0 < -1$$

and

$$F_{\frac{1}{2}}(s) = 2\pi \operatorname{cosec} 2\pi(s+1) \quad \text{with} \quad -\tfrac{3}{2} < \sigma_0 < -1.$$

Substituting the above into (2.15) gives

$$\overline{\psi}_2 = \frac{-\tfrac{1}{2}\pi \cos(\phi - \tfrac{1}{2}\pi) \sin(s+1)(\phi - \tfrac{1}{2}\pi)}{\sin \tfrac{1}{2}\pi(s+1) \cos \tfrac{1}{2}s\pi}$$

and

$$\overline{\psi}_{\frac{1}{2}} = \frac{-2\pi \cos(\phi - \tfrac{1}{2}\pi) \sin(s+1)(\phi - \tfrac{1}{2}\pi)}{\sin 2\pi s \cos \tfrac{1}{2}s\pi}.$$

Summing the residues associated with the inverse Mellin transform gives

$$\psi_2(r, \phi) = -\frac{2r}{\pi} \cos(\phi - \tfrac{1}{2}\pi) \frac{\{(\ln r) r^2 \sin 2(\phi - \tfrac{1}{2}\pi) + (\phi - \tfrac{1}{2}\pi)(r^2 \cos 2(\phi - \tfrac{1}{2}\pi) - r^4)\}}{1 - 2r^2 \cos 2(\phi - \tfrac{1}{2}\pi) + r^4}$$

and

$$\psi_{\frac{1}{2}}(r, \phi) = \cos(\phi - \tfrac{1}{2}\pi)$$
$$\times \frac{\{-(1-r^2) r^2 \sin(\phi - \tfrac{1}{2}\pi) + 2\pi^{-1}[r^3 (\ln r) \sin 2(\phi - \tfrac{1}{2}\pi) + (\phi - \tfrac{1}{2}\pi)\{r^3 \cos 2(\phi - \tfrac{1}{2}\pi) + r^5\}]\}}{1 + 2r^2 \cos 2(\phi - \tfrac{1}{2}\pi) + r^4}$$
$$+ 2^{\frac{1}{2}} r \frac{\{-r^{\frac{5}{2}} \sin \tfrac{3}{2}(\phi - \tfrac{1}{2}\pi) - r^{\frac{7}{2}} \sin \tfrac{1}{2}(\phi - \tfrac{1}{2}\pi) + r^{\frac{1}{2}} \sin \tfrac{1}{2}(\phi - \tfrac{1}{2}\pi) + r^{\frac{3}{2}} \sin \tfrac{3}{2}(\phi - \tfrac{1}{2}\pi)\}}{1 + 2r^2 \cos 2(\phi - \tfrac{1}{2}\pi) + r^4}$$

Using the explicit expressions for the stream function, we can calculate the shear stress exerted by the fluid on the plate,

$$\tau_{r\phi}\Big|_{\phi=0} = -\frac{1}{r^2} \frac{\partial^2 \psi}{\partial \phi^2}\Big|_{\phi=0},$$

and the shear force over $0 \leqslant r \leqslant R$,

$$F(R) = \int_0^R \tau_{r\phi}\Big|_{\phi=0} dr. \tag{2.16}$$

This gives the following relationships:

$$\tau_{r\phi 1}|_{\phi=0} = \frac{4}{\pi} r^3 \frac{(-1 + r^{-2} + 2r^{-2} \ln r)}{(r^2 - 1)^2}, \tag{2.17a}$$

$$\tau_{r\phi 2}|_{\phi=0} = \frac{4}{\pi} r^3 \frac{(-1 - r^{-2} - 2r^{-2} \ln r)}{(r^2 + 1)^2}, \tag{2.17b}$$

$$\tau_{r\phi \frac{1}{2}}|_{\phi=0} = \frac{4}{\pi} r^3 \frac{(-1 + r^{-2} + 2r^{-2} \ln r)}{(r^2 - 1)^2} - \frac{r^{-\frac{1}{2}}(1-r)}{(1+r)^2} \tag{2.17c}$$

and

$$F_1 = \frac{2}{\pi} \frac{R^2}{1 - R^2} \ln R^2, \quad F_2 = -\frac{2}{\pi} \frac{R^2}{1 + R^2} \ln R^2,$$

$$F_{\frac{1}{2}} = \frac{2}{\pi} \frac{R^2}{1 - R^2} \ln R^2 - \frac{2R^{\frac{1}{2}}}{1 + R}.$$

3. The shape of the free surface

The terms on the right-hand side of (2.12) are evaluated for each of the flow fields derived above. The following notation is adopted: $\{\phi_i,\ P_i(\infty,\ \frac{1}{2}\pi;\ B),\ f_i | i = 1, 2, \frac{1}{2}\}$ denotes the functions ϕ_{010}, P_{010} $(\infty,\ \frac{1}{2}\pi;\ B)$ and

$$2r^{-1}\{\partial v_{000}/\partial\phi + u_{000}\} - P_{010} + P_i$$

corresponding to the stream functions ψ_1, ψ_2 and $\psi_{\frac{1}{2}}$, respectively. Equation (2.12) becomes

$$d^2h_i/dr^2 - Bh_i = f_i - P_i(\infty, \tfrac{1}{2}\pi; B) \quad (i = 1, 2, \tfrac{1}{2}), \tag{3.1}$$

where $h_i \equiv r\phi_i$,

$$f_1(r) = \frac{4 - 12r^2 + 4\pi^{-1}\{r^5 + 6r^3 + 5r + [6r - 2r^3]\ln r\}}{\{1 + r^2\}^3},$$

$$f_2(r) = \frac{4r}{\pi}\frac{\{-r^4 + 6r^2 - 5 - [6 + 2r^2]\ln r\}}{\{1 - r^2\}^3},$$

$$f_{\frac{1}{2}}(r) = \frac{-4 + 12r^2 + 4\pi^{-1}\{r^5 + 6r^3 + 5r + [6r - 2r^3]\ln r\}}{\{1 + r^2\}^3} + 2^{\frac{1}{2}}\frac{\{\frac{1}{2}(1 + r)(1 + 8r - 30r^2 + 8r^3 + r^4) + (1 + r^2)(1 + 3r - 3r^2 - r^3)\}}{r^{\frac{1}{2}}(1 + r^2)^3}.$$

The boundary conditions for h_i are

(i) $\lim_{r\to\infty} h_i = 0$, i.e. the contact line is located at the origin of the co-ordinate system;

(ii) $\lim_{r\to\infty} d^2h_i/dr^2 = 0$, i.e. the free surface approaches a flat horizontal plane far away from the contact line.

The latter boundary condition enables us to replace $P_i(\infty, \frac{1}{2}\pi; B)/B$ by $H_i(B)$, the vertical distance the contact line is displaced below the free surface at $r \to \infty$ *owing to the motion of the fluid*. The exact solution of (3.1) is

$$h_i(r; B) = H_i(B)\,[1 - e^{-B^{\frac{1}{2}}r}] + h_{pi}(r; B),$$

where $$h_{pi}(r; B) = -\frac{e^{-B^{\frac{1}{2}}r}}{B^{\frac{1}{2}}}\int_0^r \sinh B^{\frac{1}{2}}\xi f_i(\xi)\,d\xi - \frac{\sinh B^{\frac{1}{2}}r}{B^{\frac{1}{2}}}\int_r^\infty e^{-B^{\frac{1}{2}}\xi} f_i(\xi)\,d\xi.$$

The dynamic contribution to the contact angle is given by

$$\phi_i(0; B) = H_i(B)\,B^{\frac{1}{2}} - \int_0^\infty e^{-B^{\frac{1}{2}}\xi} f_i(\xi)\,d\xi. \tag{3.2}$$

However, it is very unlikely that the contact angle is dependent upon gravity, i.e. B. It may be helpful to recall the *static* case for guidance: in order to determine completely the shape of the interface, not only must linear momentum and mass be conserved, but the configuration of the system must correspond to that of minimum energy. It is the latter requirement which determines the value of the static contact angle; e.g. when the solid–fluid interfaces are assumed to possess

an energy per unit area then the static contact angle is given by the Young–Dupre equation, and this relationship does not involve gravity. So far, for the *dynamic* case, we have only been concerned with conserving mass and linear momentum and so no conclusion can be drawn about the dynamic contact angle. However, it seems reasonable to *assume* that the value of the *dynamic* contact angle is also independent of gravity. Upon making this assumption we are able to express (3.2) as

$$\phi_i(0) \approx -0{\cdot}54 + C_i \quad (i = 1, 2, \tfrac{1}{2})$$

and

$$H_i(B) \approx (-4/\pi B^{\frac{1}{2}}) \ln B^{\frac{1}{2}} + C_i/B^{\frac{1}{2}} \quad (i = 1, 2, \tfrac{1}{2}),$$

where $\{C_i | i = 1, 2, \frac{1}{2}\}$ are undetermined constants, and where the following approximate relationship has been used:

$$\int_0^\infty e^{-B^{\frac{1}{2}}\xi} f_i(\xi)\, d\xi \approx 0{\cdot}54 - \frac{4}{\pi} \ln B^{\frac{1}{2}} \quad (i = 1, 2, \tfrac{1}{2}),$$

valid for $B \ll 1$.

Since B, the ratio of the slip length to the meniscus length, is most likely much less than one, we shall seek an approximate analytic expression for h_i by performing an asymptotic expansion valid for $B \to 0$. However, this expansion is not uniform in r since $B \equiv 0$ can be interpreted as corresponding to the case in which the no-slip boundary condition is assumed, and it has already been established that this boundary condition gives rise to a singularity in the interfacial shape at the contact line. Thus two domains emerge, and each has associated with it an appropriate expansion for h_i and a length scale: the inner region, that immediately adjacent to the contact line, in which the viscous and capillary forces dominate, has length scale L_s; the outer region, where gravity becomes an important factor, is scaled by $(\sigma/\rho g)^{\frac{1}{2}}$. In addition, the following boundary condition is imposed: (iii) $\phi_i(0)$, the dynamic contribution to the contact angle, is considered known. With this additional boundary condition, the value of $H_i(B)$ is determined.

Inner region

A solution to (3.1) is sought of the form

$$h_i(r; B) \sim h_{iI0}(r) + \mu_1(B)\, h_{iI1}(r) + \ldots,$$

valid in the limit as $B \to 0$ and where $\mu_1(B) \to 0$ and $BH_i(B) \to 0$ as $B \to 0$. The solutions for h_{iI0} are

$$h_{1I0} = r\phi_1(0) + \frac{2r^2}{1+r^2} + \frac{4r^3 \ln r}{\pi(1+r^2)}, \quad h_{2I0} = r\phi_2(0) - \frac{4r^3 \ln r}{\pi(1-r^2)},$$

$$h_{\frac{1}{2}I0} = r\phi_{\frac{1}{2}}(0) - \frac{2r^2}{1+r^2} + \frac{4r^3 \ln r}{\pi(1+r^2)} + \frac{2^{\frac{3}{2}} r^{\frac{3}{2}}(1+r)}{(1+r^2)}.$$

In all cases $h_{iI0} \sim r\phi_i(0) + 4\pi^{-1} r \ln r$ as $r \to \infty$ ($h_{\frac{1}{2}I0}$ has an additional term which is unbounded in the limit as $r \to \infty$); in other words, $h_{iI0} \to \infty$ as $r \to \infty$. Without the influence of gravity h_{iI0} does not approach a constant as $r \to \infty$.

Outer region

In this region the appropriate independent variable is $\hat{r} \equiv rB^{\frac{1}{2}}$. An asymptotic expansion for h_i is assumed to have the form

$$h_i(\hat{r}; B) \sim \nu_0(B)\, h_{i\phi 0}(\hat{r}) + B^{-\frac{1}{2}} h_{i\phi 1}(\hat{r}) + \ldots$$

and

$$H_i(B) \sim \nu_0(B)\, H_{i0} + B^{-\frac{1}{2}} H_{i1},$$

where $B^{-\frac{1}{2}}/\nu_0(B) \to 0$ as $B \to 0$. The lowest-order mode $h_{i\phi 0}$ satisfies

$$d^2 h_{i\phi 0}/d\hat{r}^2 - h_{i\phi 0} = -H_{i0},$$

subject to the boundary condition $\lim_{\hat{r}\to\infty} h_{i\phi 0} = H_{i0}$. Hence we have $h_{i\phi 0} = Ae^{-\hat{r}} + H_{i0}$. The equation governing the next mode is

$$d^2 h_{i\phi 1}/d\hat{r}^2 - h_{i\phi 1} = 4/\pi\hat{r} - H_{i1},$$

subject to the boundary condition $\lim_{\hat{r}\to\infty} h_{i\phi 1} = H_{i1}$. The solution is

$$h_{i\phi 1} = \frac{-4}{\pi}\left\{\sinh\hat{r}\int_{\hat{r}}^{\infty}\frac{e^{-\xi}}{\xi}\,d\xi + e^{-\hat{r}}\int_0^{\hat{r}}\frac{\sinh\xi}{\xi}\,d\xi\right\} + Ce^{-\hat{r}} + H_{i1}.$$

The constants A and C and the gauge function $\nu_0(B)$ are determined by matching the outer with the inner solution.

Matching

Since the inner solution becomes unbounded as $\nu \to \infty$, the solutions are matched by assuming that there exists an intermediate region in which both solutions are valid. This region is characterized by the variable $\hat{r} \equiv r\eta(B) = \hat{r}B^{-\frac{1}{2}}\eta(B)$, where *ord* $(B^{\frac{1}{2}})$ < *ord* (η) < 1 as $B \to 0$. Matching terms of different orders gives

$$A = -H_{i0}, \quad \nu_0(B) = \frac{4}{\pi B^{\frac{1}{2}} H_{i0}}\ln\left(\frac{1}{B^{\frac{1}{2}}}\right), \quad C = -H_{i1}, \quad \phi_i(0) = \frac{4}{\pi}(\gamma - 1) + H_{i1}$$

($\gamma \approx 0{\cdot}577216$, Euler's constant). The solutions can be expressed in the form of an expansion uniformly valid for $0 \leqslant r < \infty$ by adding together the inner and outer expansions and subtracting the common part:

$$h_1 \cong \frac{2r^2}{1+r^2} - \frac{4r\ln r}{\pi(1+r^2)} + \frac{1}{B^{\frac{1}{2}}}[e^{-rB^{\frac{1}{2}}} - 1]\left[\frac{4}{\pi}(\ln B^{\frac{1}{2}} + (\gamma - 1)) - \phi_1(0)\right]$$
$$- \frac{4}{B^{\frac{1}{2}}\pi}\left\{\sinh B^{\frac{1}{2}}r\int_{B^{\frac{1}{2}}r}^{\infty}\frac{e^{-\xi}}{\xi}\,d\xi + e^{-B^{\frac{1}{2}}r}\int_0^{B^{\frac{1}{2}}r}\frac{\sinh\xi}{\xi}\,d\xi\right\},$$

$$h_2 \cong \frac{-4r\ln r}{\pi(1-r^2)} + \frac{1}{B^{\frac{1}{2}}}[e^{-rB^{\frac{1}{2}}} - 1]\left[\frac{4}{\pi}(B^{\frac{1}{2}} + (\gamma - 1)) - \phi_2(0)\right]$$
$$- \frac{4}{B^{\frac{1}{2}}\pi}\left\{\sinh B^{\frac{1}{2}}r\int_{B^{\frac{1}{2}}r}^{\infty}\frac{e^{-\xi}}{\xi}\,d\xi + e^{-B^{\frac{1}{2}}r}\int_0^{rB^{\frac{1}{2}}}\frac{\sinh\xi}{\xi}\,d\xi\right\},$$

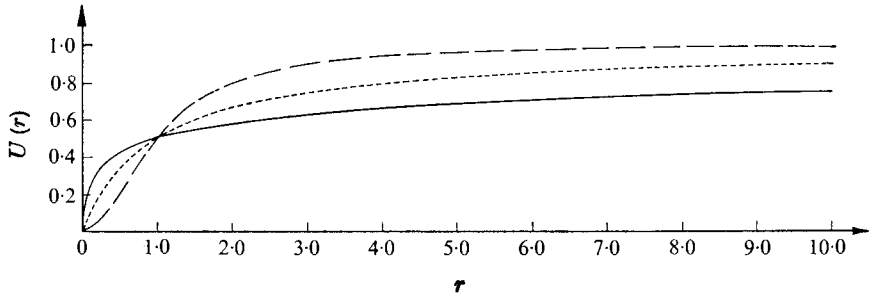

FIGURE 2. The speed of the fluid along the plate.
– – –, U_1; — —, U_2; ——, $U_{\frac{1}{2}}$.

$$h_{\frac{1}{2}} \approx -\frac{2r^2}{1+r^2} - \frac{4r\ln r}{\pi(1+r^2)} + \frac{2^{\frac{3}{2}}r^{\frac{1}{2}}(r-1)}{1+r^2}$$
$$+ B^{-\frac{1}{2}}[e^{-B^{\frac{1}{2}}r}-1][4\pi^{-1}(\ln B^{\frac{1}{2}}+\gamma-1) - \phi_{\frac{1}{2}}(0) + B^{\frac{1}{2}}(2\pi)^{\frac{1}{2}}]$$
$$- \frac{4}{B^{\frac{1}{2}}\pi}\left\{\sinh B^{\frac{1}{2}}r \int_{B^{\frac{1}{2}}r}^{\infty} \frac{e^{-\xi}}{\xi}\,d\xi + e^{-B^{\frac{1}{2}}r}\int_0^{B^{\frac{1}{2}}r} \frac{\sinh\xi}{\xi}\,d\xi\right\}$$
$$+ \frac{1}{2^{\frac{1}{2}}B^{\frac{1}{4}}}\left\{\sinh B^{\frac{1}{2}}r \int_{B^{\frac{1}{2}}r}^{\infty} \frac{e^{-\xi}}{\xi^{\frac{3}{2}}}\,d\xi + e^{-B^{\frac{1}{2}}r}\int_0^{B^{\frac{1}{2}}r} \frac{\sinh\xi}{\xi^{\frac{3}{2}}}\,d\xi\right\}.$$

In the expression for $h_{\frac{1}{2}}$ the outer solution is presented up to $O(B^{-\frac{1}{4}})$. The solutions for H_i are

$$H_i \cong \frac{4}{\pi B^{\frac{1}{2}}}\ln\left(\frac{1}{B^{\frac{1}{2}}}\right) + \frac{1}{B^{\frac{1}{2}}}\left(\phi_i(0) + \frac{4}{\pi}(1-\gamma)\right) \quad \text{for} \quad i = 1, 2,$$
$$H_{\frac{1}{2}} \approx \frac{4}{\pi B^{\frac{1}{2}}}\ln\left(\frac{1}{B^{\frac{1}{2}}}\right) + \frac{1}{B^{\frac{1}{2}}}\left(\phi_{\frac{1}{2}}(0) + \frac{4}{\pi}(1-\gamma) - B^{\frac{1}{4}}(2\pi)^{\frac{1}{2}}\right).$$

4. Results

The velocity fields derived in the previous section can be compared on the slip length scale and on the meniscus length scale. From the point of view of the slip length scale they are quite different. First, the rate at which $U(r)$ approaches zero as $r \to 0$ is different, i.e.

$$\lim_{r\to 0} dU/dr = \begin{cases} 1 & (i = 1), \\ 0 & (i = 2), \\ \infty & (i = \frac{1}{2}); \end{cases}$$

see figure 2. The tangential component $\tau_{r\phi_i}|_{\phi=0}$, of the surface traction vector evaluated at the wall also differs quite a bit; see figure 3. For $i = 1, 2$, $\tau_{r\phi_i}|_{\phi=0}$ approaches zero as $r \to 0$ (note the switch in sign for $i = 2$); however, for $i = \frac{1}{2}$ the stress becomes unbounded. The force F, given by (2.16), also differs among the various models (see figure 4), although $F(0) = 0$ even for the case $i = \frac{1}{2}$. On the other hand, the dynamic contribution h_i to the interfacial shape is quite similar for all three slip models; see figure 5.

While many differences exist on the slip length scale, few, if any, are perceptible on the meniscus length scale. In all three cases

$$U \to 1, \quad \tau_{r\phi}|_{\phi=0} \sim -4/\pi r, \quad F \sim -4\pi^{-1}\ln R \quad \text{as} \quad r, R \to \infty,$$

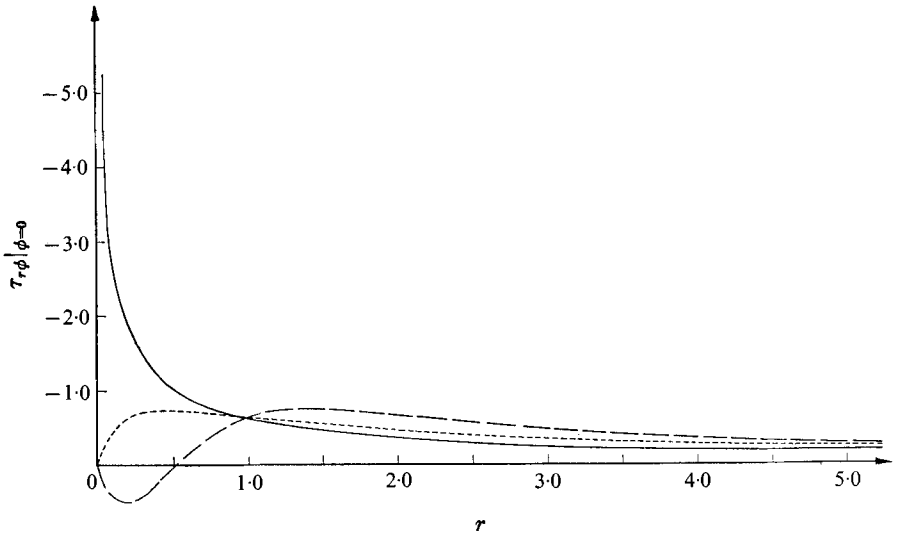

FIGURE 3. The tangential component of the surface traction vector evaluated at various positions along the plate. Curves as in figure 2.

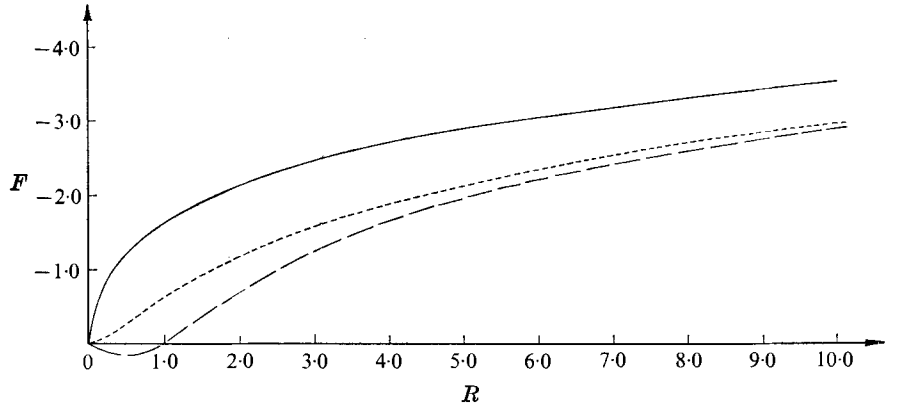

FIGURE 4. The tangential component of the force exerted by the fluid on the plate from the contact line to a position R. Curves as in figure 2.

and

$$H(B) \approx \frac{-4}{\pi B^{\frac{1}{2}}} \ln B^{\frac{1}{2}} + \frac{1}{B^{\frac{1}{2}}} \left\{ \phi_{010}(0) + \frac{4}{\pi}(1-\gamma) \right\}$$

as long as $B \ll 1$. In addition, all three models give rise to the same interfacial shape h_i; see figure 6. Nevertheless, all of these quantities *are* sensitive to the magnitude of the slip length L_s. Since this seems to be the only characteristic of the slip model which affects the flow on the meniscus length scale, a solution is included in the appendix in which α can take on any value between 0 and π (exclusive). This particular solution coincides with the case $i = 1$ when $\alpha = \frac{1}{2}\pi$.

All of the above-mentioned quantities come directly from solutions to the second-order problem. Hence, in order to express the dynamic contact angle, or

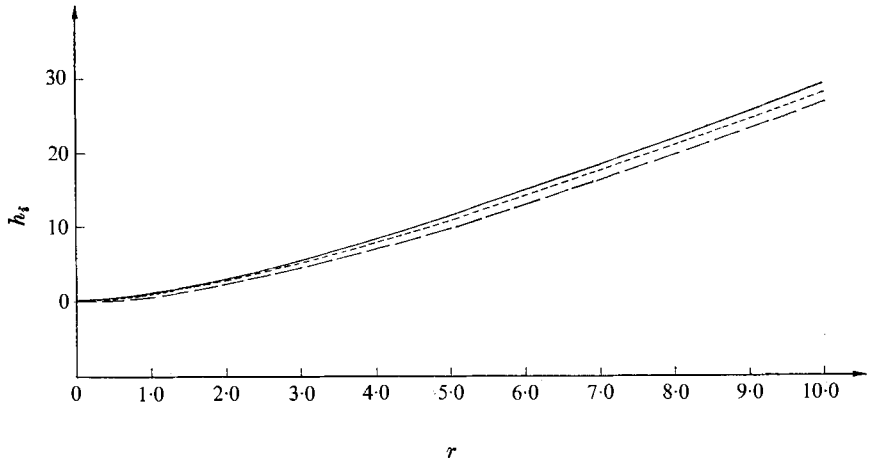

FIGURE 5. The shape of the free surface viewed on the slip length scale for the three slip models. It is assumed that $\{\phi_i(0) = 0 | i = 1, 2, \frac{1}{2}\}$. – – –, $i = 1$; ——, $i = 2$; ——, $i = \frac{1}{2}$.

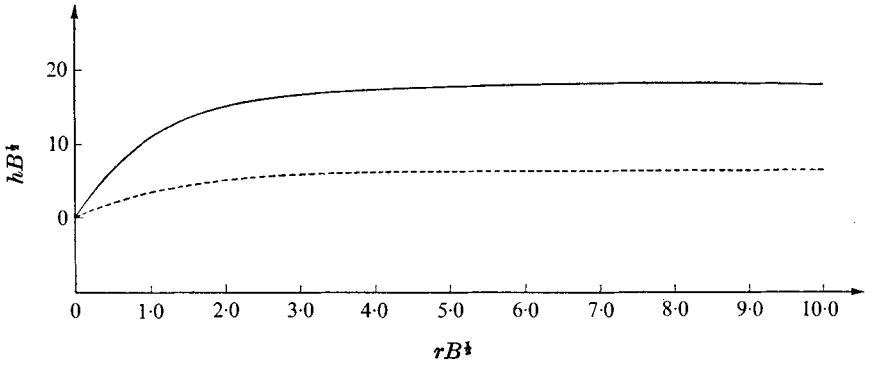

FIGURE 6. The shape of the free surface viewed on the meniscus length scale for two extreme values of the slip length. – – –, $B^{\frac{1}{2}} = 10^{-2}$; ——, $B^{\frac{1}{2}} = 10^{-6}$.

the vertical displacement of the contact line below the asymptotic level of the free surface as $r \to \infty$, the entire expansion must be used, i.e.

$$\phi(0) \sim \phi_s + C\phi_{010}(0),$$

$$\lim_{r\to\infty} r\phi \sim (\phi_s - \alpha)/B^{\frac{1}{2}} + CH(B).$$

It has tacitly been assumed that the slip lengths associated with the different slip models are the same. It is not at all obvious what criterion should be used to compare them. For instance, if

$$L_A \sim L_B \quad \Leftrightarrow \quad \int_0^\infty (1-U_A)^2\,dr = \int_0^\infty (1-U_B)^2\,dr$$

is used then the value of the slip length associated with $U_{\frac{1}{2}}$ is not well defined because the integral does not exist. Until a more precise criterion based on some

physical principle can be established, the following attitude will be taken: the slip lengths appearing in the above three models are equivalent because they all predict the same $F(R)$, $\tau_{r\phi}|_{\phi=0}$ and $H(B)$ on the meniscus length scale.

5. Discussion and conclusions

In order to remove the singularity at the moving contact line, while simultaneously retaining a Newtonian model for the fluid, it has been established (Dussan V. & Davis 1974) that the velocity field must be continuous at the contact line. This implies, for the specific geometry considered above, that the velocity of the fluid at the contact line is zero. On the other hand, owing to the impressive success of the no-slip boundary condition in predicting flow fields under 'normal' conditions, it seems appropriate to assume that the fluid approaches this condition away from the contact line. Hence the speed $U(r)$ of the fluid at the wall must have the following characteristics:

$$\text{(i)} \lim_{r\to 0} U(r) = 0, \quad \text{(ii)} \lim_{r\to\infty} U(r) = 1,$$

when the dimensionless speed of the wall is 1. However, the form of $U(r)$ in the intermediate region, i.e. the region in which U increases from 0 to 1, is not at all obvious. One might inquire as to the extent to which this region affects the overall velocity field. To investigate this point, we have examined in detail the flow field associated with three different slip boundary conditions. These were chosen specifically because of their behaviour as $r\to 0$. Since condition (i) removes a singularity, it was thought that this particular set of boundary conditions, each possessing a vastly different value of dU/dr at $r = 0$, would be the most likely to illustrate the sensitivity of the entire flow field to the functional form of $U(r)$. The diversity within this set can be established from another point of view. One might think that a rational approach for posing a slip boundary condition is

$$\tau_{r\phi}|_{\phi=0} = f(U-1), \tag{5.1}$$

where the explicit form of the function f depends on the physical properties of the fluid and solid. More specifically, it has been suggested (Goldstein 1965) that f should be a linear function, i.e.

$$\tau_{r\phi}|_{\phi=0} = \bar{\beta}(U-1), \tag{5.2}$$

where $\bar{\beta}$, a constant, is called the slip coefficient. The three slip models investigated in the previous section can be interpreted in terms of the above in two different ways. First, in order to make a direct comparison with (5.2), β_i, a 'local slip coefficient' defined by

$$\beta_i \equiv \tau_{r\phi i}|_{\phi=0}/(U_i(r)-1) \quad (i = 1, 2, \tfrac{1}{2}),$$

is evaluated along the wall. Each case behaves differently: $\beta_1 = 0$ at $r = 0$ and approaches a constant value as $r\to\infty$; $\beta_2 = 0$ at $r = 0$ and tends to infinity as $r\to\infty$ ($\beta_2 \sim 4r/\pi$ as $r\to\infty$); $\beta_{\frac{1}{2}} = -\infty$ at $r = 0$, becomes positive at $r \approx 3$ and tends to zero as $r\to\infty$; refer to figure 7. Also, the function $f(U-1)$, appearing in

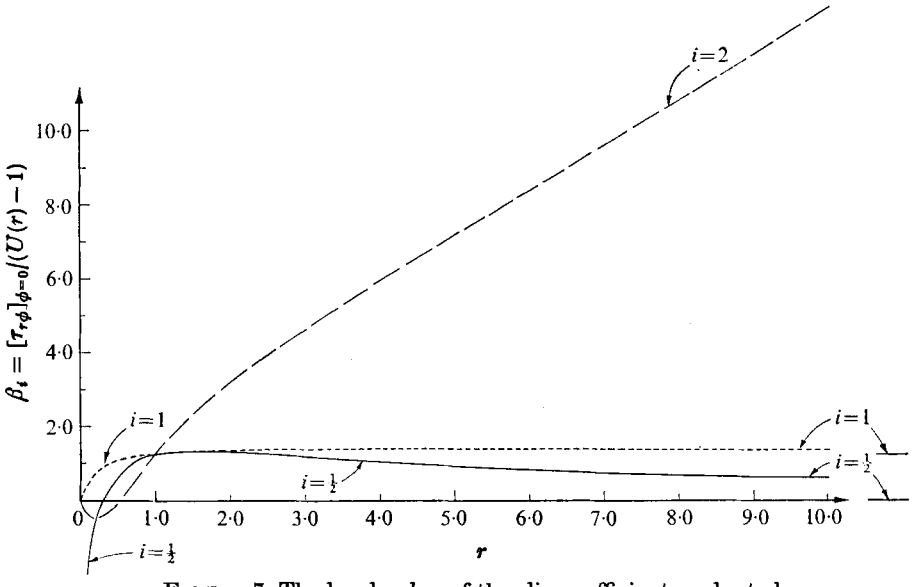

FIGURE 7. The local value of the slip coefficient evaluated for the three slip models.

(5.1) can be determined for each slip model. This is accomplished by replacing r in (2.17) by the function $r(U-1)$ given by

$$r(U-1) \equiv \begin{cases} -U/(U-1) & (i=1), \\ [-U/(U-1)]^{\frac{1}{2}} & (i=2), \\ [-U/(U-1)]^{2} & (i=\frac{1}{2}); \end{cases}$$

refer to figure 8. Since it has already been established that $U(r)$ must obey conditions (i) and (ii), it follows that f evaluated in the region as $1-U \to 0$ applies to the flow at large r, i.e. away from the moving contact line, where the fluid is asymptotically approaching the no-slip condition; while f evaluated as $1-U \to 1$ applies to the flow in the slip region. It is interesting to note that not only do these slip models differ near the contact line but they also possess a vastly different behaviour away from the contact line, i.e. as $r \to \infty$ we have $\beta_1 \to$ constant, $\beta_2 \to \infty$ and $\beta_{\frac{1}{2}} \to 0$. In spite of these differences it was shown in the previous section that, upon examining the characteristics of their corresponding velocity fields on the meniscus length scale, they all appear the same. Hence a fluid mechanician who does not make observations on a length scale less than about a micrometre will find it difficult to distinguish between some vastly different slip models.

There is, however, one characteristic which at least distinguishes $U_{\frac{1}{2}}$ from U_1 and U_2. The velocity field associated with $U_{\frac{1}{2}}$ has the property that $|\nabla \mathbf{u}| \to \infty$ as $r \to 0$. This in itself does not make it noteworthy: even though it gives rise to an unbounded stress tensor at $r = 0$, the physically relevant quantities such as force and interfacial shape remain well defined. What makes this case different is the fact that the contact line is *not a material line*. That is to say, a material point initially located on the fluid interface reaches the contact line in a

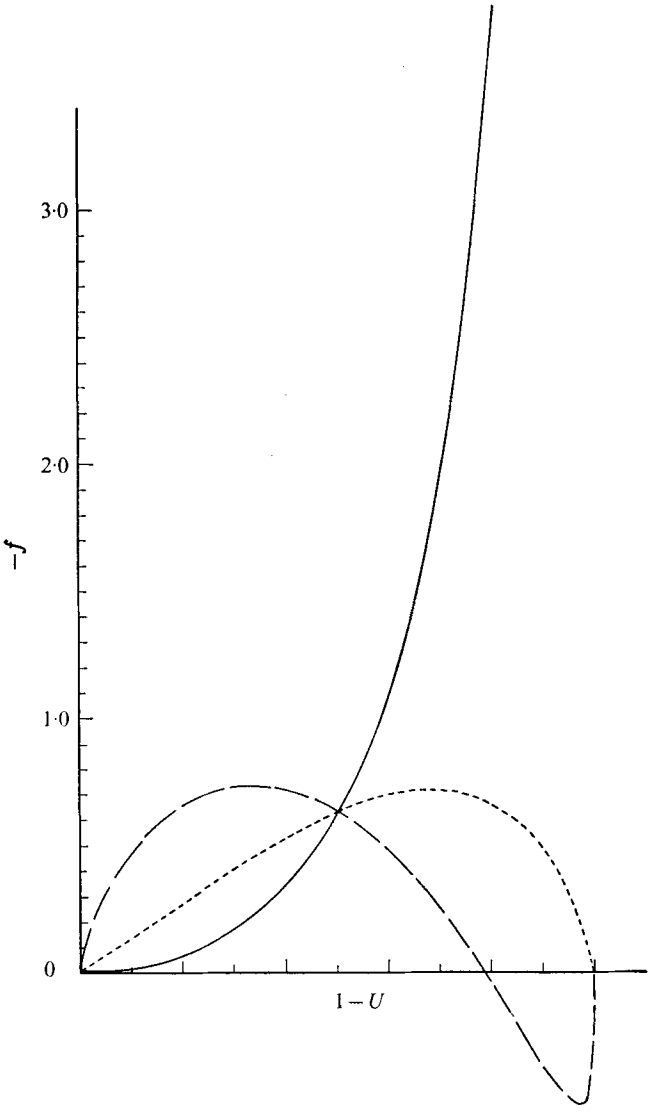

FIGURE 8. The slip function corresponding to the three slip models. – – –, $i = 1$; ——, $i = 2$; ——, $i = \frac{1}{2}$.

finite interval of time; once at the contact line, it moves along the solid–fluid interface in the direction of the motion of the wall. Hence the solid–fluid interface is *not* a fluid material surface. On the other hand, for U_1 and U_2 the contact line is a material line and the solid–fluid interface always consists of the same fluid material points (it is necessary but not sufficient that $|\nabla \mathbf{u}| \to \infty$ as $r \to 0$; for a discussion on the differences between bounding surfaces and material surfaces refer to Dussan V. 1976). Hence, if one is interested in the situation in which a surface-active agent is present on the fluid interface then one might be somewhat concerned with the functional form of $U(r)$: the motion associated with

$U_{\frac{1}{2}}$ will cause the surface-active agent to coat the walls, while the other models will not have this characteristic.

Over the past 150 years much effort has gone into the study of static menisci, with a significant portion focused on the static contact angle. A vast amount of experimental data has been collected on the value of the static contact angle for different fluid–fluid–solid systems (Jasper 1972). Hence it is not surprising to find that almost all experimental studies on the *moving* contact line heavily emphasize measuring the dependence of the *dynamic* contact angle on the speed of the contact line, e.g. Ablett (1923), Yarnold & Mason (1949), Rose & Heins (1962), Schonhorn, Frisch & Kwei (1966), Elliot & Riddiford (1967), Schwartz & Tejada (1972) and Hoffman (1975). However, upon comparing figure 5 with figure 6, it can be concluded that measuring the dynamic contact angle may be difficult owing to the rapid variation in the shape of the interface close to the contact line. On the slip length scale (figure 5), it is evident that $\phi_{010}(0) = 0$ (this gives a 90° contact angle); but on the meniscus length scale (figure 6), the dynamic contribution to the contact angle appears to be positive with a magnitude dependent on the speed of the contact line (recall that the ordinate of figure 6 must be multiplied by $U_0\mu/(\sigma g\rho)^{\frac{1}{2}}$ to make it dimensional). Hansen & Toong (1971) draw the same conclusion on the basis of their analysis of a liquid displacing a gas through a circular capillary tube. They find that the shape of the interface undergoes a rapid change very close to the moving contact line. (They handle the singularity by ignoring the flow field within a domain of radius l_0 surrounding the moving contact line. Any boundary condition needed is applied to the outer surface of this domain. The reported rapid change in the shape of the interface occurs outside but close to the ignored region.) In addition to the fact that the above-mentioned experimental studies are most likely reporting apparent contact angles, *it is not at all obvious that these measurements are independent of the overall configuration of the materials, i.e. that the measurements depend only on the properties of the materials involved.*

Removing the singularity at the moving contact line by using a slip boundary condition has introduced *two* parameters: the slip length L_s and the dynamic contribution $C\phi_{010}(0)$ to the contact angle. One could derive expressions for these quantities based on a more detailed knowledge of the displacement process. For example, one may use molecular models (Hansen & Miotto 1957) or continuum models based on events taking place on the submicron length scale where the moving contact line may appear very unsteady owing to the roughnesses in the solid surface, in which small quantities of fluid may become trapped. In this case it might make sense to interpret $C\phi_{010}$ and L_s as statistically averaged quantities. On the other hand, one could examine flow fields in different geometries and evaluate $C\phi_{010}$ and L_s by comparing experimental observations with analyses. This approach may prove to be sufficient from a fluid-mechanical point of view since it has been shown here that the overall flow field is rather insensitive to the details of the slip model. However, for this to be successful, i.e. for the use of a slip boundary condition to remove the singularity, the L_s and $C\phi_{010}$ so determined must be independent of the geometry of the experiment used to evaluate them.

I am grateful to both Stephen Davis and Fred Kafka for their numerous and always spirited discussions in which all of our ideas flowed freely, and to the National Sciences Foundation, Engineering Mechanics Program, for its support through grants GK 40714 and ENG 74–10297.

Appendix

Since the overall flow does not seem to be sensitive to the details in the slip model near the contact line, a solution is presented for a specific slip model in which α may vary between 0 and π.

The speed of the fluid along the wall is assumed to have the form

$$U(r;\alpha) = \frac{2\alpha r^{\pi/2\alpha}}{2\alpha - \sin 2\alpha}\left\{\frac{(-r^{\pi/2\alpha}+1+\ln r^{\pi/2\alpha})\sin 2\alpha}{2\alpha[r^{\pi/2\alpha}-1]^2} + \frac{1}{r^{\pi/2\alpha}+1}\right\}.$$

Evaluating $F(s;\alpha)$ gives

$$F(s;\alpha) = \frac{4\alpha^2}{2\alpha-\sin 2\alpha}\frac{\{-(s+1)\sin 2\alpha + \sin[(s+1)2\alpha]\}}{\sin^2[(s+1)2\alpha]},$$

which yields

$$\bar{\psi}(s,\phi;\alpha) = \frac{4\alpha^2}{2\alpha-\sin 2\alpha}\frac{\{\sin s\alpha \sin(s+2)(\phi-\alpha) - \sin(s+2)\alpha \sin s(\phi-\alpha)\}}{\sin^2[(s+1)2\alpha]}.$$

Evaluating the inverse Mellin transformation by summing residues gives

$$\begin{aligned}
&\psi(r,\phi;\alpha)\frac{[2\alpha-\sin 2\alpha]}{2} \\
&= r^{1-2\pi/\alpha}\frac{[\alpha\cos\alpha\sin(\phi-\alpha)-(\phi-\alpha)\sin\alpha\cos(\phi-\alpha)][1+r^{\pi/\alpha}\cos[(\phi-\alpha)\pi/\alpha]]}{1+2r^{-\pi/\alpha}\cos[(\phi-\alpha)\pi/\alpha]+r^{-2\pi/\alpha}} \\
&\quad + \frac{r^{1-\pi/\alpha}(\ln r)\sin\alpha\cos(\phi-\alpha)\sin[(\phi-\alpha)\pi/\alpha]}{1+2r^{-\pi/\alpha}\cos[(\phi-\alpha)\pi/\alpha]+r^{-2\pi/\alpha}} \\
&\quad - \frac{r^{1-\pi/\alpha}[\alpha\sin\alpha\cos(\phi-\alpha)-(\phi-\alpha)\cos\alpha\sin(\phi-\alpha)][1-r^{-\pi/\alpha}]\sin[(\phi-\alpha)\pi/2\alpha]}{1+2r^{-\pi/\alpha}\cos[(\phi-\alpha)\pi/\alpha]+r^{-2\pi/\alpha}} \\
&\quad + \frac{r^{1-\pi/\alpha 2}(\ln r)\cos\alpha\sin(\phi-\alpha)\cos[(\phi-\alpha)\pi/2\alpha][1+r^{-\pi/\alpha}]}{1+2r^{-\pi/\alpha}\cos(\phi-\alpha)\pi/\alpha+r^{-2\pi/\alpha}} \\
&\quad - r[\alpha\cos\alpha\sin(\phi-\alpha)-(\phi-\alpha)\sin\alpha\cos(\phi-\alpha)].
\end{aligned}$$

REFERENCES

Ablett, R. 1923 An investigation of the angle of contact between paraffin wax and water. *Phil. Mag.* **46**, 244.

Bascom, W. D., Cottington, R. L. & Singleterry, C. R. 1964 Dynamic surface phenomena in the spontaneous spreading of oils on solids. In *Contact Angles, Wettability, and Adhesion* (ed. R. E. Gould), p. 355. Washington, D.C.: Am. Chem. Soc.

Dussan, V., E. B. 1976 On the differences between a bounding surface and a material surface. *J. Fluid Mech.* **75**, 609.

Dussan, V., E. B. & Davis, S. H. 1974 On the motion of a fluid–fluid interface along a solid surface. *J. Fluid Mech.* **65**, 71.

Elliot, G. E. P. & Riddiford, A. A. 1967 Dynamic contact angles. I. The effect of impressed motion. *J. Colloid Interface Sci.* **23**, 389.

GOLDSTEIN, S. 1965 Note on the conditions at the surface of contact of a fluid with a solid body. In *Modern Development in Fluid Mechanics*, vol. 2, p. 676. Dover.

HANSEN, R. J. & TOONG, T. Y. 1971 Dynamic contact angle and its relationship to forces of hydrodynamic origin. *J. Colloid Interface Sci.* **37**, 196.

HANSEN, R. S. & MIOTTO, M. 1957 Relaxation phenomena and contact angle hysteresis. *J. Am. Chem. Soc.* **79**, 1765.

HOFFMAN, R. L. 1975 A study of the advancing interface. I. Interface shape in liquid–gas systems. *J. Colloid Interface Sci.* **50**, 228.

HUH, C. & SCRIVEN, L. E. 1971 Hydrodynamic model of steady movement of a solid liquid/fluid contact line. *J. Colloid Interface Sci.* **35**, 85.

JASPER, J. J. 1972 *J. Phys. Chem. Ref.* **1**, 841.

JOHNSON, R. E. & DETTRE, R. H. 1964 Contact angle hysteresis. I. Study of an idealized rough surface. II. Contact angle measurements on rough surfaces. In *Contact Angles, Wettability, and Adhesion* (ed. R. E. Gould), p. 112. Washington, D.C.: Am. Chem. Soc.

LOPEZ, J., MILLER, C. A. & RUCKENSTEIN, E. 1976 Spreading kinetics of liquid drops on solids. *J. Colloid Interface Sci.* **56**, 460.

LUDVIKSSON, V. & LIGHTFOOT, E. N. 1968 Deformation of advancing menisci. *A.I.Ch.E. J.* **14**, 674.

MORSE, P. M. & FESHBACH, H. 1953 *Methods of Theoretical Physics*, part I. McGraw-Hill.

ROSE, W. & HEINS, R. W. 1962 Moving interfaces and contact angle rate-dependency. *J. Colloid Sci.* **17**, 39.

SCHONHORN, H., FRISCH, H. L. & KWEI, T. K. 1966 Kinetics of wetting of surfaces by polymer melts. *J. Appl. Phys.* **37**, 4967.

SCHWARTZ, A. M. & TEJADA, S. B. 1972 Studies of dynamic contact angle on solids. *J. Colloid Interface Sci.* **38**, 359.

TRANTER, C. J. 1948 The use of the Mellin transform in finding the stress distribution in an infinite wedge. *Quart. J. Mech. Appl. Math.* **1**, 125.

YARNOLD, G. D. & MASON, B. J. 1949 The angle of contact between water and wax. *Proc. Phys. Soc.* **B62**, 125.

ZISMAN, W. A. 1964 Relation of equilibrium contact angle to liquid and solid constitution. In *Contact Angles, Wettability, and Adhesion* (ed. R. E. Gould), p. 1. Washington, D.C.: Am. Chem. Soc.